Imaging Lenticular Autofluorescence in Older Subjects

Jason Charng,[1] Rose Tan,[2,3] Chi D. Luu,[2,3] Sam Sadigh,[1] Dwight Stambolian,[1] Robyn H. Guymer,[2,3] Samuel G. Jacobson,[1] and Artur V. Cideciyan[1]

[1]Scheie Eye Institute, Perelman School of Medicine, University of Pennsylvania, Philadelphia, Pennsylvania, United States
[2]Centre for Eye Research Australia, Royal Victorian Eye and Ear Hospital, East Melbourne, Victoria, Australia
[3]Department of Surgery (Ophthalmology), The University of Melbourne, Parkville, Victoria, Australia

Correspondence: Artur V. Cideciyan, Scheie Eye Institute, 51 North 39th Street, Philadelphia, PA 19104, USA; cideciya@pennmedicine.upenn.edu.

Submitted: July 3, 2017
Accepted: August 29, 2017

Citation: Charng J, Tan R, Luu CD, et al. Imaging lenticular autofluorescence in older subjects. *Invest Ophthalmol Vis Sci*. 2017;58:4940–4947. DOI:10.1167/iovs.17-22540

Purpose. To evaluate whether a practical method of imaging lenticular autofluorescence (AF) can provide an individualized measure correlated with age-related lens yellowing in older subjects undergoing tests involving shorter wavelength lights.

Methods. Lenticular AF was imaged with 488-nm excitation using a confocal scanning laser ophthalmoscope (cSLO) routinely used for retinal AF imaging. There were 75 older subjects (ages 47–87) at two sites; a small cohort of younger subjects served as controls. At one site, the cSLO was equipped with an internal reference to allow quantitative AF measurements; at the other site, reduced-illuminance AF imaging (RAFI) was used. In a subset of subjects, lens density index was independently estimated from dark-adapted spectral sensitivities performed psychophysically.

Results. Lenticular AF intensity was significantly higher in the older eyes than the younger cohort when measured with the internal reference (59.2 ± 15.4 vs. 134.4 ± 31.7 gray levels; $P < 0.05$) as well as when recorded with RAFI without the internal reference (10.9 ± 1.5 vs. 26.1 ± 5.7 gray levels; $P < 0.05$). Lenticular AF was positively correlated with age; however, there could also be large differences between individuals of similar age. Lenticular AF intensity correlated well with lens density indices estimated from psychophysical measures.

Conclusions. Lenticular AF measured with a retinal cSLO can provide a practical and individualized measure of lens yellowing, and may be a good candidate to distinguish between preretinal and retinal deficits involving short-wavelength lights in older eyes.

Keywords: aging, AMD, lens density, night vision, pre-retinal absorption, psychophysics, quantitative autofluorescence, reduced-illuminance autofluorescence imaging, RAFI, scotopic testing

Age-related macular degeneration (AMD) is a multifactorial disease with major genetic and environmental contributions.[1] One of the characteristics of early AMD is dysfunction of the rod-photoreceptor–mediated scotopic function. Another characteristic of AMD is abnormal accumulations found in and around the retinal pigment epithelium (RPE) cells, which normally contain lipofuscin. Thus, scotopic function testing and lipofuscin imaging of the RPE are promising approaches currently investigated for the detection of earliest disease stages and predicting progression.[2–6] Importantly, both approaches tend to use shorter wavelength lights. One of the impediments to performing quantitative measurements of retinal function and structure in an aged population with short wavelength lights is the preretinal light absorption, which can vary between individuals and generally increases with age.[7,8]

The dominant contributor to the preretinal absorption of short-wavelength light is the age-related yellowing of the lens.[9–11] The human lens is comprised of mostly water and protein[12] and photo-oxidation over time leads to structural changes in the proteins,[13] which subsequently results in accumulation of tissue-bound, advanced glycation end products (AGEs) in the lens.[14–19] Accrual of AGEs in the lens has been demonstrated to decrease light transmission through the lens.[20–24] In particular, it has been shown that such reduction in light transmittance preferentially affects the short wavelength portion of the visible spectrum.[25] Natural fluorophores of the lens also accumulate with age and this can be measured noninvasively.[14,20,21,26–29] In the current study, we investigated the feasibility of imaging lenticular autofluorescence (L-AF) with a standard confocal scanning laser ophthalmoscope (cSLO) routinely used for retinal AF imaging, and using the L-AF intensity as an index of lens density in older subjects.

Methods

Human Subjects

The studies were performed at two sites: Centre for Eye Research Australia (Site 1) and Scheie Eye Institute at the University of Pennsylvania (Site 2). Initial studies were performed and completed in Site 2. Based on preliminary analyses of findings at Site 2, a larger study was designed at Site 1 to take advantage of the quantitative AF (qAF) technique available there. The main populations included at both Sites were older subjects (Site 1: $n = 51$, age range 47–87 years; Site 2: $n = 24$, age range 48–84 years). In addition, a limited set of younger control subjects was also enrolled (Site 1: $n = 6$, age range 29–37 years; Site 2: $n = 5$, age range 24–29 years). In Site 1, 25 eyes had no apparent aging changes in the retina, 23 had intermediate AMD, 1 early AMD, and 2 late AMD with

noncentral geographic atrophy using the clinical classification criteria.[30] In terms of the anterior segment, no opacification was detected in 22 eyes and 29 eyes showed mild to moderate cataractous changes according to the World Health Organization grading system,[31] which distinguishes three main types of cataract (cortical [C], nuclear [N], and posterior subcapsular [PSC]) into three severities (1, 2, or 3). Of the 29 eyes, 15 had C1 only; 7 had N1 only; 1 had C2 only; 1 had N2 only; 1 had C1+N1; 1 had C2+N1; and, 3 had C1+N1+PSC1. In Site 2, 22 eyes had intermediate AMD while two subjects showed no or minimal aging changes. Seven eyes had no lenticular opacities whereas 17 eyes were diagnosed with cataractous changes (15 with N1 only; 1 with N2 only; 1 with C1+N1). None of the subjects at either site had diabetes. The study eye was the one with the better visual acuity to ensure greater stability of fixation during the tomography measurements especially relevant for the subset of patients with early AMD and to select for eyes with smaller opacities. Right eyes were selected in cases with equal visual acuity. Pupils were dilated before all recordings. All procedures adhered to the tenets of the Declaration of Helsinki and informed consent was obtained from all subjects.

Lenticular Autofluorescence Imaging Using an Internal Reference

At Site 1, a cSLO (Spectralis HRA+OCT; Heidelberg Engineering, Heidelberg, Germany) modified to include an internal fluorescence reference[32] was used to acquire qAF images of the anterior segment including the lens. Before the start of recording, the focus of the cSLO was preset to a fixed value of +45 diopters (D) and kept invariant. Using the infrared reflectance mode, the camera was shifted along all three axes until the iris was brought into focus without modifying the focus setting. After acquiring a single frame, short-wavelength AF mode (488-nm excitation; laser power 100%, sensitivity 67%; 30° lens) was turned on and optical sectioning was performed under the tomography mode. There were 64 frames obtained over 8 mm (maximum range available) to sample the three-dimensional volume of the anterior segment including the lens. Following the acquisition of the tomograph, infrared reflectance mode was switched back on to ensure that the iris had remained in focus and another frame was acquired.

To analyze each qAF z-stack, scans from each eye were exported as a series of 64 bitmap images (768 × 850 pixels) and were imported into ImageJ software (http://imagej.nih.gov/ij/; provided in the public domain by the National Institutes of Health, Bethesda, MD, USA). Lenticular qAF (L-qAF) profile was calculated using the following equation, which was adopted from previous work[32]:

$$\text{L-qAF} = \frac{GL_L - GL_0}{GL_R - GL_0} \quad (1)$$

where GL_L refers to the mean gray level of a 60 × 60-pixel region placed near the pupil center of each image within the z-stack. GL_0 is the black level provided by the software for the first frame of the z-stack; there was minimal variation of GL_0 across subjects at Site 1 (SD = 0.72 gray levels). In some eyes, GL_L sample location was moved slightly off-center to avoid central opacity. GL_R is the gray level corresponding to the internal fluorescence reference. To calculate GL_R, a 200 × 18-pixel region of interest was placed in the internal fluorescence reference area and mean gray level was calculated on each image of a z-stack. The GL_R value used in Equation 1 was the maximum value recorded within each z-stack.

Lenticular Autofluorescence Imaging Without an Internal Reference

At Site 2, a cSLO (Spectralis HRA; Heidelberg Engineering) without an internal fluorescence reference was used to acquire AF images of the anterior eye including the lens. Subject preparation, equipment setup, and data analysis were similar to that performed in Site 1 with three differences. First, reduced-illuminance AF imaging (RAFI)[33] was used (laser power = 25%, sensitivity = 65%; 30° lens). Second, the focus of the cSLO was preset to a fixed value of +40 D and kept invariant. Third, L-AF was calculated using the following equation:

$$\text{L-AF} = GL_L - GL_0 \quad (2)$$

where GL_L denotes the mean gray level of a 60 × 60-pixel region placed near the pupil center; GL_0 was the black level provided by the software for the first frame of the z-stack; there was minimal variation of GL_0 across subjects at Site 2 (SD = 1.27 gray levels). Note that Equation 2 is simply the numerator in Equation 1.

Perceptual Lens Density Measurement

Lens density index was estimated perceptually in 18 of 24 older eyes at Site 2 and compared with L-AF imaging. First, scotopic sensitivity spectrum of each dark-adapted eye was estimated by sampling sensitivities with 420-, 500-, 560-, and 650-nm stimuli (Goldmann V diameter, 200-ms duration) using previously published methods.[34] Testing was performed at 18° in the inferior field, near the rod hot-spot.[35] The resultant sensitivities were fit to a scotopic sensitivity spectrum S(λ) that explicitly accounts for individual differences in lens density using a simple model[36]:

$$S(\lambda) = \text{RHO}(\lambda) + k \cdot \text{TL1}(\lambda) + \text{TL2}(\lambda) \quad (3)$$

where RHO(λ) represents the human rhodopsin absorption spectrum.[37,38] TL1(λ) represents the lens transmission component 1; TL2(λ) represents the lens transmission component 2. S(λ), RHO(λ), TL1(λ), and TL2(λ) were specified in log units. Each subject's set of scotopic sensitivities were fit by S(λ) allowing the scale factor, k, to vary by minimizing the sum-of-square merit function using the Solver module in Excel (Microsoft, Redmond, WA, USA). Perceptual lens density index was calculated from S(λ) fit at λ = 490 nm (i.e., k × TL1[490] + TL2[490]) for each subject and compared to the peak L-AF intensity measured at 488 nm in the same subject.

Results

Quantitative Autofluorescence of the Lens: Depth-Resolved Imaging

The geometry between the cSLO camera and the anterior eye was first set up by visualization of the dilated iris in focus with infrared reflectance mode (Fig. 1A). Next, volumetric AF imaging was performed by switching to short-wavelength AF imaging in tomography mode and acquiring 64 frames representing the optical sections of the fluorescence intensity originating from natural fluorophores (Fig. 1B). Sectioning was performed starting from approximately 2.5-mm anterior to the iris focal plane over an 8-mm axial distance posteriorly (Fig. 1A). Stability of the camera-eye geometry during the recording was confirmed with the acquisition of a repeated iris reflectance image following the tomography mode. Representative z-stack images demonstrate the gradual increase in AF intensity followed by the gradual decrease along the anterior

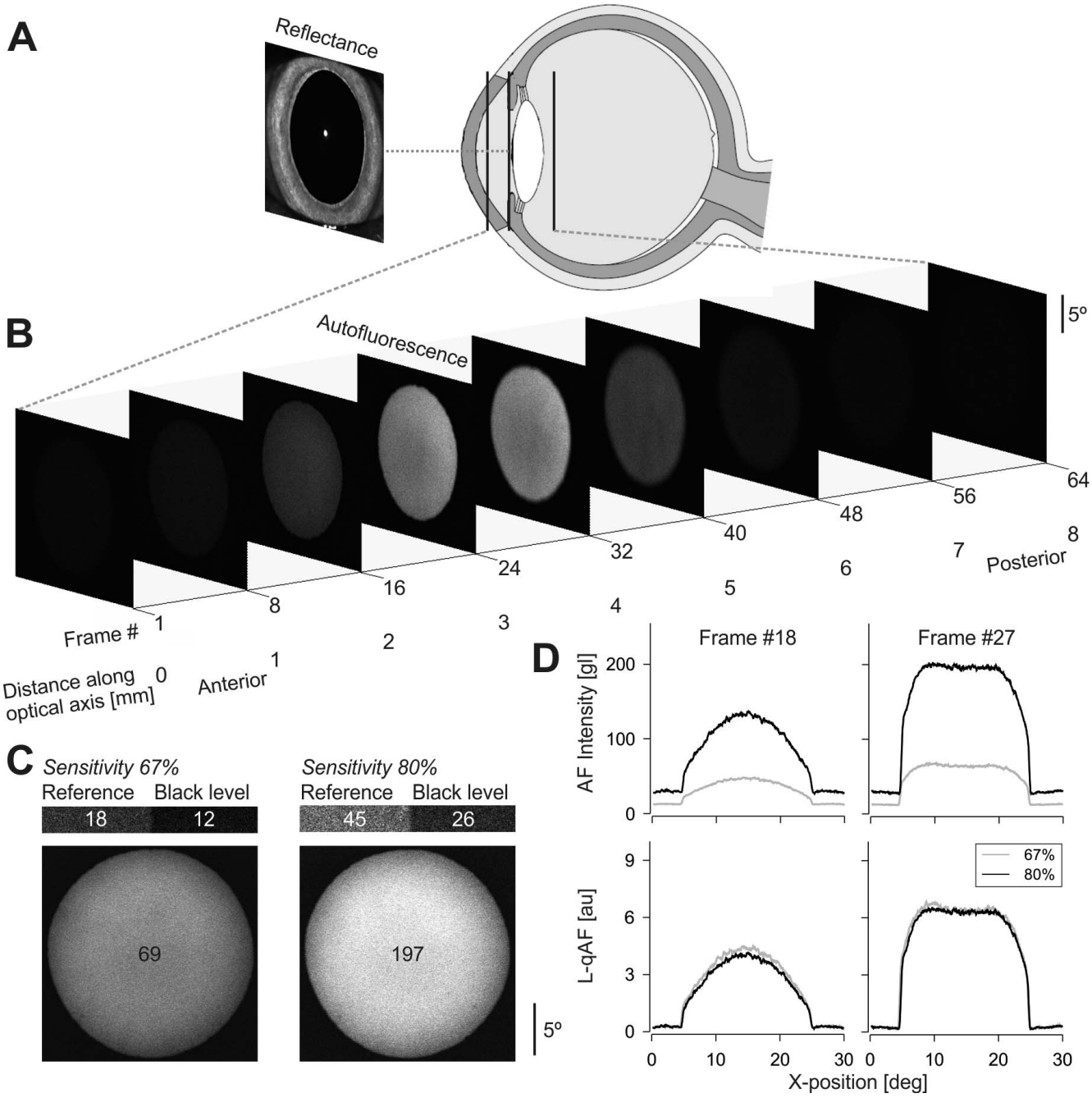

FIGURE 1. Depth-resolved quantitative autofluorescence (qAF) imaging of the human lens. (**A**, **B**) A confocal scanning laser ophthalmoscope is first focused on the iris in infrared reflectance mode (**A**), and then optical sectioning tomography (64 slices) is performed over 8-mm depth from anterior to posterior direction using AF imaging with short-wavelength (488 nm) excitation (**B**). Autofluorescence intensity increases as the focal plane moves from the anterior segment to the middle of the lens; there is a decline in intensity as the focus shifts toward posterior lens. (**C**, **D**) Representative results in a subject obtained with two sensitivity settings to evaluate the range of linearity and saturation. Lenticular qAF (L-qAF) images at frame #27 (corresponding to peak intensity) and the corresponding calibration reference and black level images; numbers represent the raw gray level values averaged over a 60 × 60-pixel region at pupil center and 200 × 18-pixel regions for the reference and black level (**C**). Plots show AF intensity as raw gray level values as a function of distance along the horizontal axis (*upper plot*), and the corresponding L-qAF calculation (*lower plot*) at frames #18 and #27. The results generated by the two sensitivity settings become nearly identical after conversion from raw gray levels to L-qAF.

posterior axis over a depth of approximately 5 mm, which is likely dominated by the lenticular fluorophores (Fig. 1B).

In order to confirm that the internal fluorescence reference originally designed for qAF imaging of the retina[32] could also be used for lenticular imaging, L-AF images were acquired with two sensitivity settings (Fig. 1C). In a representative young eye, the sensitivity setting of 67% resulted in 69, 18, and 12 gray levels (gl) for maximal GL_L, reference, and black level, respectively. With the 80% sensitivity setting, on the other hand, the respective values were 197, 45, and 26 gl. Lenticular AF values across horizontal profiles at two selected frames show the expected differences due to sensitivity setting (Fig. 1D, upper). However conversion of raw L-AF values to L-qAF with the use of Equation 1 demonstrated the wide range of linearity of the instrument in this imaging geometry for the anterior eye (Fig. 1D, lower).

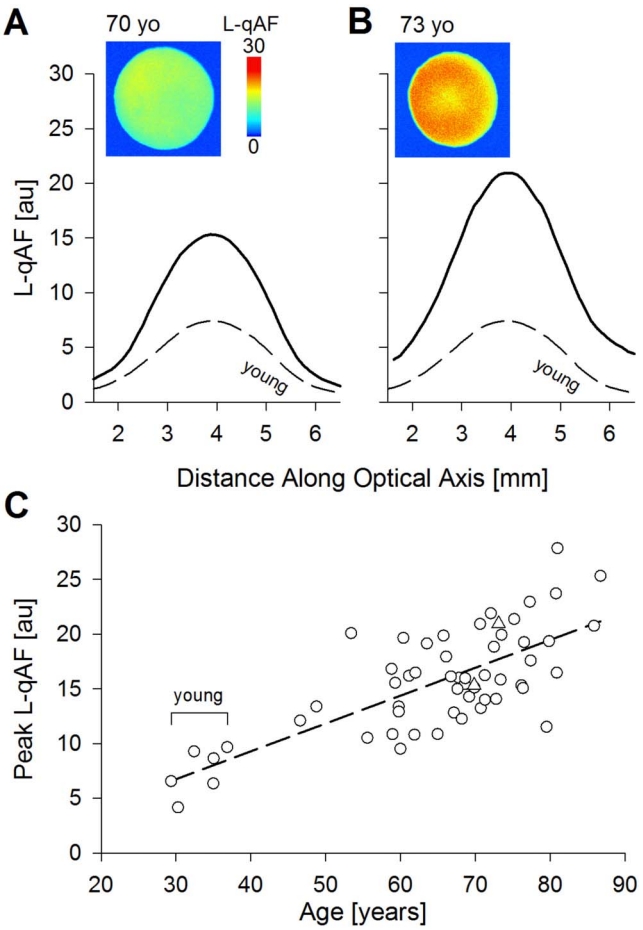

FIGURE 2. Lenticular quantitative autofluorescence (L-qAF). (**A**, **B**) Lenticular qAF (L-qAF) in two representative older eyes (ages 70, 73) of similar age plotted against distance along optical axis (*black lines*) shows single-peaked curves with different maximal values. *Dashed lines* show the average L-qAF in younger eyes. *Insets*, peak L-AF frames for each eye on a pseudocolor scale. (**C**) Lenticular qAF values plotted against age. *Dashed line* depicts the linear regression fit to the whole cohort. *Triangles* indicate the two representative subjects shown in (**A**, **B**).

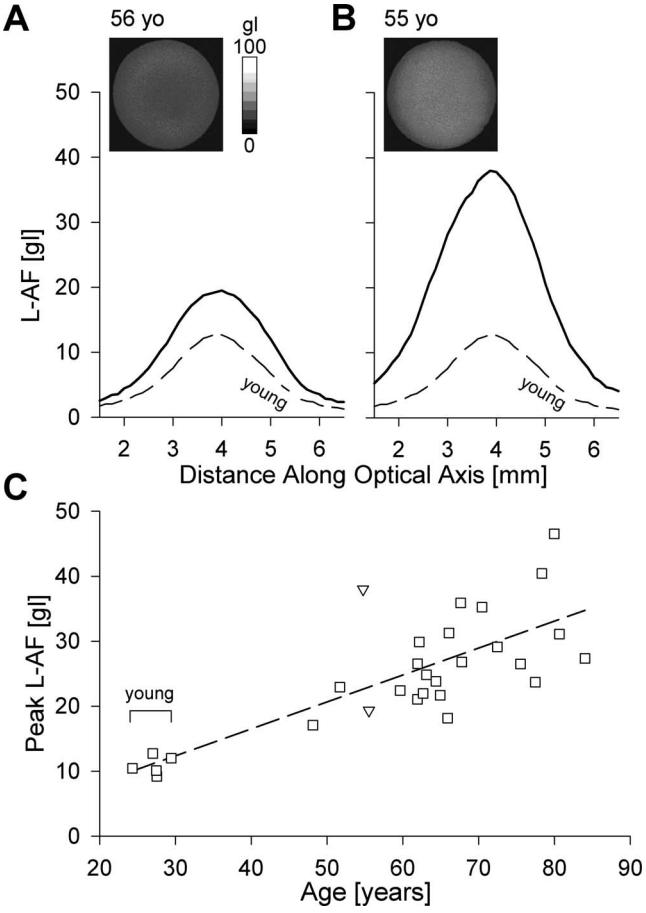

FIGURE 3. Lenticular autofluorescence without the internal fluorescence reference. (**A**, **B**) Lenticular autofluorescence (L-AF) imaging in two representative older eyes (ages 56, 55) of similar age plotted against distance along optical axis (*solid black lines*) show higher intensities compared with the average of younger eyes (*dashed line*). *Insets*, peak L-AF frames for both older eyes on an adjusted gray scale to allow visualization. (**C**) Lenticular autofluorescence values plotted against age. *Dashed line* depicts the linear regression fit to the whole cohort. *Triangles* indicate the two representative subjects shown in (**A**, **B**).

Next, we examined the relationship between L-qAF and age. Two representative older subjects in the eighth decade of life can show quite different L-qAF images at their peak focal plane (Fig. 2A, 2B, insets). Lenticular qAF sampled near the center of the lens as a function of distance along the optical axis (z-axis) peaked at 15.3 arbitrary units (au) (Fig. 2A) and 20.9 au (Fig. 2B), which were both substantially higher than the mean of younger eyes. As a cohort, L-AF and L-qAF intensities were significantly higher in the older eyes than the younger eyes (134.4 ± 31.7 vs. 59.2 ± 15.4 gl; $P < 0.05$; 16.6 ± 4.0 vs. 7.4 ± 2.1 au; $P < 0.05$; ages 47–87 years vs. 29–37 years, respectively). The z-axis location of the peak was not different between older and younger eyes (3.04 ± 0.30 vs. 3.12 ± 0.47 mm; $P = 0.69$). The relationship between L-qAF and age showed a positive linear correlation (L-qAF [au] = 0.25 × Age [y] − 0.91; $R^2 = 0.54$). Importantly, there was a large variation in L-qAF among subjects of similar age (Fig. 2C).

Measuring Lenticular Autofluorescence Without an Internal Reference

Considering the potential concern that bright imaging lights might have an effect on accelerating retinal disease,[39] we used a cSLO with reduced laser power to perform lenticular RAFI[33] without an internal fluorescence reference. In two representatives in the sixth decade of life, peak L-AFs (Fig. 3A, 19.3 gl; Fig. 3B, 38.0 gl) were higher when compared with the young eyes. As a cohort, L-AF intensities were significantly higher in the older eyes than the younger eyes (26.1 ± 5.7 vs. 10.9 ± 1.5 gl; $P < 0.05$). The z-axis location of the peak was not different between older and younger eyes (3.15 ± 0.16 vs. 3.42 ± 0.38 mm; $P = 0.14$). When L-AF obtained with RAFI was plotted against age (Fig. 3C), there was a positive linear correlation (L-AF [gl] = 0.41 × Age [y] − 0.06; $R^2 = 0.60$). Importantly, L-AF variation was also present across individuals of similar age as it was observed with L-qAF.

Lens Density Index From Scotopic Spectral Sensitivity: Comparison With Lenticular Autofluorescence

Lens density is the dominant contributor to preretinal absorption of shorter wavelength lights. In order to obtain an independent assessment of lens density, we took advantage of rod-photoreceptor–mediated vision under dark-adapted conditions in a subset (18/24) of older eyes with L-AF

measurements. The spectral sensitivity function under scotopic conditions was assumed to be dominated by the sum of three components: two (RHO and TL2) are invariant, and one (TL1) varies for each individual (Fig. 4A). Spectral sensitivities in two representative older individuals of similar age demonstrate how individual spectra can vary from the standard scotopic luminosity function (V_λ') due to differences in light absorption in the shorter wavelength region (Fig. 4B). The cohort of older subjects showed perceptual lens density indices ranging from 0.21 to 0.63 log. Peak L-AF intensities showed an approximately monotonic relationship with lens density indices (at 490 nm) estimated from scotopic sensitivity functions (Fig. 4C; Peak L-AF [gl] = 34.05 × perceptual lens density [log] + 11.42; $R^2 = 0.59$). A log-linear relationship would be consistent with the hypothesis that the measured peak L-AF intensity (and thus the maximum concentration of lenticular fluorophores) is proportional to the maximum concentration of absorbing pigments in the lens, and thus correlate with logarithm of absorbance estimated by the perceptual lens density index.

Discussion

Functional or structural evaluations of the retina or RPE with shorter wavelength lights are confounded by preretinal absorption, which is generally related to age but tends to vary between subjects. Age-related lenticular yellowing is one of the dominant contributors to preretinal absorption, which has been previously estimated by objective and perceptual methods. Objective methods have included comparing relative intensities of the third and the fourth Purkinje images,[40] measuring only the intensity of the fourth Purkinje image,[41,42] calculating the ratio between posterior and anterior AF intensities of the lens,[21,43] or determining the amount of back-scattered light using Scheimpflug photography combined with densitometric image analysis.[44] Perceptual methods have taken advantage of the scotopic spectral sensitivity curve[2,36] as well as measuring color matching function.[45] All of these methods either use specialized equipment or require extensive testing time. Here, we strived for a simple and practical method using a cSLO commonly available in retina clinics to image lenticular AF. We collected three-dimensional lenticular AF data set of the anterior eye including the lens. We assumed that the peak L-AF intensity is monotonically related to lenticular yellowing[20,27] and that there is minimal AF contribution from the cornea due to the confocal imaging system employed. Once confirmed by a wider data set, routine L-AF imaging could contribute practical individualized information regarding lens density in older subjects.

Previous in vivo studies have consistently reported a positive correlation between maximum L-AF and age in eyes with no significant cataract.[20,29,46–49] The relationship has been described as linear over broad[20,29,46] and narrow[47] age ranges, or exponentially increasing over broad[48] and narrow[49] age ranges. Some studies were performed with commercial fluorophotometers[20,29,46,47,49] others with custom-built equipment.[48] The data from the current study are consistent with a definite increase in L-AF intensity with age, however, the exact shape of the relationship requires greater numbers of subjects distributed throughout the age ranges.

The aging lens undergoes a spectrum of alterations that include yellowing and opacification that incrementally decrease the transmission of external light to the retina.[11,50,51] Our results are consistent with the hypothesis that L-AF increases with age-related yellowing; however, lenticular opacifications are expected to correspond to a paradoxical decrease in L-AF intensity.[20,27] Thus use of L-AF intensity as an index of lens density may not be applicable to eyes with dense cataract, which was not included in the current cohort. Lens density index based on perceptual methods, on the other hand, would be applicable to the full range of opacifications. However, a major limitation of perceptual methods is the

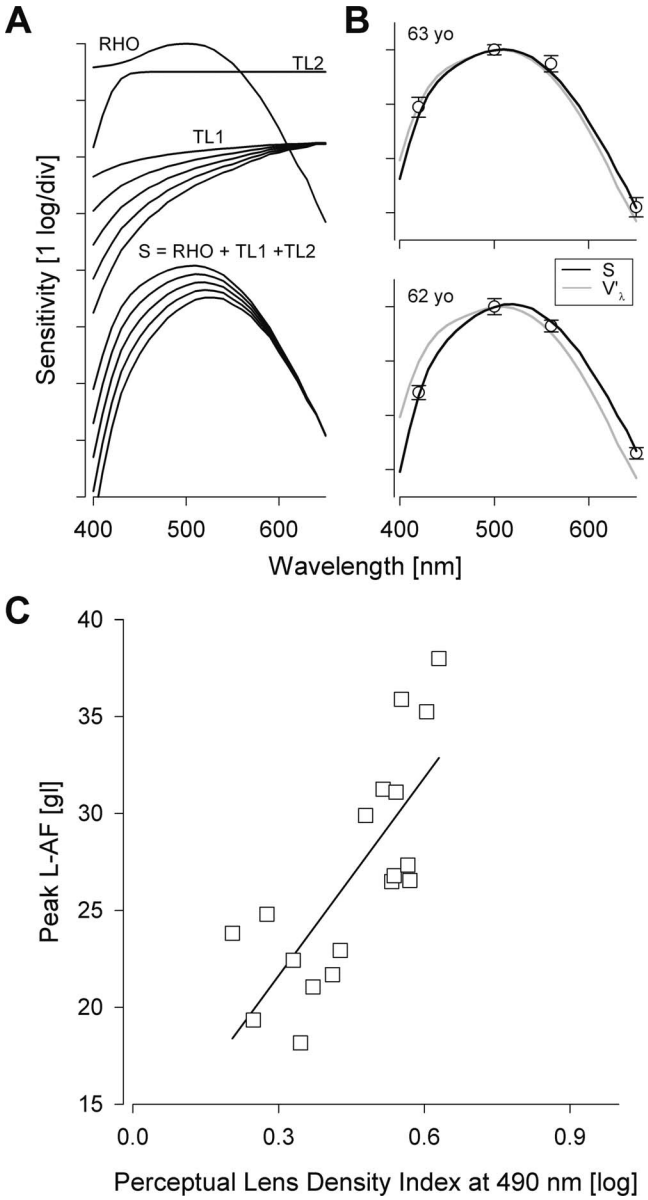

Figure 4. Correlation of perceptual lens density index with lenticular autofluorescence (L-AF). (**A**) Psychophysical estimation of lens density index involves consideration of the spectral sensitivity of rhodopsin (RHO), lens transmission component 1 (TL1), and lens transmission component 2 (TL2). Both RHO and TL2 sensitivity were held invariant among subjects, whereas TL1 was scaled individually for each subject to adjust the spectral shape. S representing the sum of RHO, TL1, and TL2 shows the expected changes in the scotopic sensitivity spectrum as a function of the scaling parameter. (**B**) Dark-adapted spectral sensitivity functions (*solid lines*) in two representative subjects estimated from sensitivities assessed at 420, 500, 560, and 650 nm (*circles*, average ± SD). Shown is a 63-year-old with a lower lens density index (*upper*) compared with another subject of similar age with a higher lens density index (*lower*). *Gray lines* depict the standard scotopic luminosity function. (**C**) Lenticular autofluorescence peak intensity [gl] plotted against perceptual lens density estimates obtained from scotopic sensitivity values [log]. Regression line is shown.

requirement that enough rod function exists across the different colored stimuli used to obtain the spectral sensitivity function. Patients with AMD and inherited retinal degenerations often have compromised rod function.[2,52,53] It is thus important to consider the population of interest before deciding on a method to estimate preretinal absorption of light.

Two types of z-axis (axial) profiles have been previously reported for lenticular AF: two-peaked profiles[20–22,26,27,43] versus single-peaked profiles.[19,29] Our results using a retinal cSLO generated a single-peaked profile (Figs. 2, 3). The source of the profile differences is not known but could include the properties of the excitation light. The current work used a narrow spectrum 488-nm excitation light. It is likely that different fluorophores that accumulate in the lens with age have not only different excitation spectra[14,19] but also different axial distribution.[54] Thus, L-AF measurements using a wider spectrum may be expected to excite different fluorophores compared with those using a narrow spectrum.

Abnormal RPE lipofuscin levels, which have been implicated in the pathology of many retinal diseases,[3,55–58] can be noninvasively measured with AF imaging.[59,60] It has thus become important to compare RPE lipofuscin levels between patients, between eyes, and monitor changes over time to examine the natural history of disease or to evaluate outcomes of therapeutic interventions. Reproducible measurements with AF imaging can be achieved by attempting to keep all imaging system variables constant[33,61] or with the use of an internal fluorescence standard, which is imaged simultaneously with the retina using qAF mode.[5,32,62–65] It is important to note that neither approach corrects for differences in preretinal absorption of excitation (and emission) lights in each individual. Quantitative AF imaging uses a correction based on the age of the subject, which is satisfactory but not ideal. The current work with L-qAF imaging provides a practical approach to individualized correction of retinal qAF values for preretinal absorption differences with a minimal additional imaging time and no extra equipment beyond what is required for retinal qAF imaging.

Acknowledgments

Supported by grants from the Pennsylvania Department of Health (Philadelphia, PA, USA), Macula Vision Research Foundation (Philadelphia, PA, USA), Beckman Initiative for Macular Research (Irvine, CA, USA), Foundation Fighting Blindness (Columbia, MD, USA), Research to Prevent Blindness (New York, NY, USA), National Eye Institute (EY001583; Bethesda, MD, USA), Macular Disease Foundation Australia (Melbourne, VIC, Australia), The National Health and Medical Research Council (NHMRC) Australia - Project Grant (#1084081; Canberra, ACT, Australia), The NHMRC Principal Research Fellowship (Canberra, ACT, Australia). The Centre for Eye Research Australia receives Operational Infrastructure Support from the Victorian Government.

Disclosure: **J. Charng**, None; **R. Tan**, None; **C.D. Luu**, None; **S. Sadigh**, None; **D. Stambolian**, None; **R.H. Guymer**, None; **S.G. Jacobson**, None; **A.V. Cideciyan**, None

References

1. Sobrin L, Seddon JM. Nature and nurture- genes and environment- predict onset and progression of macular degeneration. *Prog Retin Eye Res*. 2014;40:1–15.
2. Owsley C, Jackson GR, Cideciyan AV, et al. Psychophysical evidence for rod vulnerability in age-related macular degeneration. *Invest Ophthalmol Vis Sci*. 2000;41:267–273.
3. Holz FG, Steinberg JS, Gobel A, Fleckenstein M, Schmitz-Valckenberg S. Fundus autofluorescence imaging in dry AMD: 2014 Jules Gonin lecture of the Retina Research Foundation. *Graefes Arch Clin Exp Ophthalmol*. 2015;253:7–16.
4. Fraser RG, Tan R, Ayton LN, Caruso E, Guymer RH, Luu CD. Assessment of retinotopic rod photoreceptor function using a dark-adapted chromatic perimeter in intermediate age-related macular degeneration. *Invest Ophthalmol Vis Sci*. 2016;57:5436–5442.
5. Gliem M, Muller PL, Finger RP, McGuinness MB, Holz FG, Charbel Issa P. Quantitative fundus autofluorescence in early and intermediate age-related macular degeneration. *JAMA Ophthalmol*. 2016;134:817–824.
6. Owsley C, Clark ME, McGwin G Jr. Natural history of rod-mediated dark adaptation over 2 years in intermediate age-related macular degeneration. *Trans Vis Sci Technol*. 2017;6(3):15.
7. Gunkel RD, Gouras P. Changes in scotopic visibility thresholds with age. *Arch Ophthalmol*. 1963;69:4–9.
8. Johnson CA, Adams AJ, Lewis RA. Evidence for a neural basis of age-related visual field loss in normal observers. *Invest Ophthalmol Vis Sci*. 1989;30:2056–2064.
9. Chylack LT Jr, Ransil BJ, White O. Classification of human senile cataractous change by the American Cooperative Cataract Research Group (CCRG) method: III. The association of nuclear color (sclerosis) with extent of cataract formation, age, and visual acuity. *Invest Ophthalmol Vis Sci*. 1984;25:174–180.
10. Mellerio J. Yellowing of the human lens: nuclear and cortical contributions. *Vision Res*. 1987;27:1581–1587.
11. Bron AJ, Vrensen GF, Koretz J, Maraini G, Harding JJ. The ageing lens. *Ophthalmologica*. 2000;214:86–104.
12. Sen AC, Ueno N, Chakrabarti B. Studies on human lens: I. Origin and development of fluorescent pigments. *Photochem Photobiol*. 1992;55:753–764.
13. Goosey JD, Zigler JS Jr, Kinoshita JH. Cross-linking of lens crystallins in a photodynamic system: a process mediated by singlet oxygen. *Science*. 1980;208:1278–1280.
14. Sato K, Bando M, Nakajima A. Fluorescence in human lens. *Exp Eye Res*. 1973;16:167–172.
15. Lerman S, Kuck JF Jr, Borkman R, Saker E. Accleration of an aging parameter (fluorogen) in the ocular lens. *Ann Ophthalmol*. 1976;8:558–561.
16. Lerman S, Borkman R. Ultraviolet radiation in the aging and cataractous lens: a survey. *Acta Ophthalmol (Copenh)*. 1978;56:139–149.
17. Dillon J, Atherton SJ. Time resolved spectroscopic studies on the intact human lens. *Photochem Photobiol*. 1990;51:465–468.
18. Dyer DG, Blackledge JA, Katz BM, et al. The Maillard reaction in vivo. *Z Ernahrungswiss*. 1991;30:29–45.
19. Gakamsky A, Duncan RR, Howarth NM, et al. Tryptophan and non-tryptophan fluorescence of the eye lens proteins provides diagnostics of cataract at the molecular level. *Sci Rep*. 2017;7:40375.
20. Occhipinti JR, Mosier MA, Burstein NL. Autofluorescence and light transmission in the aging crystalline lens. *Ophthalmologica*. 1986;192:203–209.
21. Van Best JA, Kuppens EV. Summary of studies on the blue-green autofluorescence and light transmission of the ocular lens. *J Biomed Opt*. 1996;1:243–250.
22. Siik S, Chylack LT Jr, Friend J, et al. Lens autofluorescence and light scatter in relation to the lens opacities classification system, LOCS III. *Acta Ophthalmol Scand*. 1999;77:509–514.
23. van den Berg TJ, Coppens JE, van Best JA. Derivation of lenticular transmittance from fluorophotometry. *Invest Ophthalmol Vis Sci*. 2002;43:3003–3007.
24. Broendsted AE, Hansen MS, Lund-Andersen H, Sander B, Kessel L. Human lens transmission of blue light: a comparison

of autofluorescence-based and direct spectral transmission determination. *Ophthalmic Res*. 2011;46:118–124.

25. Artigas JM, Felipe A, Navea A, Fandino A, Artigas C. Spectral transmission of the human crystalline lens in adult and elderly persons: color and total transmission of visible light. *Invest Ophthalmol Vis Sci*. 2012;53:4076–4084.
26. Jacobs R, Krohn DL. Fluorescence intensity profile of human lens sections. *Invest Ophthalmol Vis Sci*. 1981;20:117–120.
27. Larsen M, Lund-Andersen H. Lens fluorometry: light-attenuation effects and estimation of total lens transmittance. *Graefes Arch Clin Exp Ophthalmol*. 1991;229:363–370.
28. Schmitt A, Schmitt J, Munch G, Gasic-Milencovic J. Characterization of advanced glycation end products for biochemical studies: side chain modifications and fluorescence characteristics. *Anal Biochem*. 2005;338:201–215.
29. Burd J, Lum S, Cahn F, Ignotz K. Simultaneous noninvasive clinical measurement of lens autofluorescence and rayleigh scattering using a fluorescence biomicroscope. *J Diabetes Sci Technol*. 2012;6:1251–1259.
30. Ferris FL III, Wilkinson CP, Bird A, et al. Clinical classification of age-related macular degeneration. *Ophthalmology*. 2013; 120:844–851.
31. Thylefors B, Chylack LT Jr, Konyama K, et al. A simplified cataract grading system. *Ophthalmic Epidemiol*. 2002;9:83–95.
32. Delori F, Greenberg JP, Woods RL, et al. Quantitative measurements of autofluorescence with the scanning laser ophthalmoscope. *Invest Ophthalmol Vis Sci*. 2011;52:9379–9390.
33. Cideciyan AV, Swider M, Aleman TS, et al. Reduced-illuminance autofluorescence imaging in ABCA4-associated retinal degenerations. *J Opt Soc Am A Opt Image Sci Vis*. 2007;24:1457–1467.
34. Cideciyan AV, Hufnagel RB, Carroll J, et al. Human cone visual pigment deletions spare sufficient photoreceptors to warrant gene therapy. *Hum Gene Ther*. 2013;24:993–1006.
35. Curcio CA, Sloan KR, Kalina RE, Hendrickson AE. Human photoreceptor topography. *J Comp Neurol*. 1990;292:497–523.
36. Pokorny J, Smith VC, Lutze M. Aging of the human lens. *Appl Opt*. 1987;26:1437–1440.
37. Wyszecki G, Stiles WS. Color Science: *Concepts and Methods, Quantitative Data and Formulae.* 2nd ed. New York: John Wiley & Sons; 1982.
38. Dartnall HJ, Bowmaker JK, Mollon JD. Human visual pigments: microspectrophotometric results from the eyes of seven persons. *Proc R Soc Lond B Biol Sci*. 1983;220:115–130.
39. Cideciyan AV, Jacobson SG, Aleman TS, et al. In vivo dynamics of retinal injury and repair in the rhodopsin mutant dog model of human retinitis pigmentosa. *Proc Natl Acad Sci U S A*. 2005;102:5233–5238.
40. Said FS, Weale RA. The variation with age of the spectral transmissivity of the living human crystalline lens. *Gerontologia*. 1959;3:213–231.
41. Johnson CA, Howard DL, Marshall D, Shu H. A noninvasive video-based method for measuring lens transmission properties of the human eye. *Optom Vis Sci*. 1993;70:944–955.
42. Savage GL, Johnson CA, Howard DL. A comparison of noninvasive objective and subjective measurements of the optical density of human ocular media. *Optom Vis Sci*. 2001; 78:386–395.
43. Zeimer RC, Noth JM. A new method of measuring in vivo the lens transmittance, and study of lens scatter, fluorescence and transmittance. *Ophthalmic Res*. 1984;16:246–255.
44. Wegener A, Laser-Junga H. Photography of the anterior eye segment according to Scheimpflug's principle: options and limitations - a review. *Clin Exp Ophthalmol*. 2009;37:144–154.
45. Stiles WS, Burch JM. N.P.L. Colour-matching investigation: final report (1958). *Opt Acta*. 1959;6:1–26.
46. Bleeker JC, van Best JA, Vrij L, van der Velde EA, Oosterhuis JA. Autofluorescence of the lens in diabetic and healthy subjects by fluorophotometry. *Invest Ophthalmol Vis Sci*. 1986;27:791–794.
47. van Wirdum E, van Best J, Bruining GJ, de Beaufort C, Oosterhuis J. Blood-retinal and blood-aqueous barrier permeability, lens autofluorescence and transmission in insulin-dependent diabetic youngsters. *Graefes Arch Clin Exp Ophthalmol*. 1989;227:26–29.
48. Siik S, Airaksinen PJ, Tuulonen A, Alanko HI, Nieminen H. Lens autofluorescence in healthy individuals. *Acta Ophthalmol (Copenh)*. 1991;69:187–192.
49. Kessel L, Kofoed PK, Zubieta-Calleja G, Larsen M. Lens autofluorescence is not increased at high altitude. *Acta Ophthalmol*. 2010;88:235–240.
50. Gaillard ER, Zheng L, Merriam JC, Dillon J. Age-related changes in the absorption characteristics of the primate lens. *Invest Ophthalmol Vis Sci*. 2000;41:1454–1459.
51. Dillon J, Zheng L, Merriam JC, Gaillard ER. Transmission of light to the aging human retina: possible implications for age related macular degeneration. *Exp Eye Res*. 2004;79:753–759.
52. Cideciyan AV, Swider M, Aleman TS, et al. ABCA4 disease progression and a proposed strategy for gene therapy. *Hum Mol Genet*. 2009;18:931–941.
53. Charng J, Cideciyan AV, Jacobson SG, et al. Variegated yet non-random rod and cone photoreceptor disease patterns in RPGR-ORF15-associated retinal degeneration. *Hum Mol Genet*. 2016;25:5444–5459.
54. Van Schaik HJ, Alkemade C, Swart W, Van Best JA. Autofluorescence of the diabetic and healthy human cornea in vivo at different excitation wavelengths. *Exp Eye Res*. 1999;68:1–8.
55. Cideciyan AV, Aleman TS, Swider M, et al. Mutations in ABCA4 result in accumulation of lipofuscin before slowing of the retinoid cycle: a reappraisal of the human disease sequence. *Hum Mol Genet*. 2004;13:525–534.
56. Sparrow JR, Boulton M. RPE lipofuscin and its role in retinal pathobiology. *Exp Eye Res*. 2005;80:595–606.
57. Boon CJ, Jeroen Klevering B, Keunen JE, Hoyng CB, Theelen T. Fundus autofluorescence imaging of retinal dystrophies. *Vision Res*. 2008;48:2569–2577.
58. Aleman TS, Soumittra N, Cideciyan AV, et al. CERKL mutations cause an autosomal recessive cone-rod dystrophy with inner retinopathy. *Invest Ophthalmol Vis Sci*. 2009;50: 5944–5954.
59. Delori FC, Dorey CK, Staurenghi G, Arend O, Goger DG, Weiter JJ. In vivo fluorescence of the ocular fundus exhibits retinal pigment epithelium lipofuscin characteristics. *Invest Ophthalmol Vis Sci*. 1995;36:718–729.
60. von Ruckmann A, Fitzke FW, Bird AC. Distribution of fundus autofluorescence with a scanning laser ophthalmoscope. *Br J Ophthalmol*. 1995;79:407–412.
61. Lois N, Halfyard AS, Bird AC, Fitzke FW. Quantitative evaluation of fundus autofluorescence imaged "in vivo" in eyes with retinal disease. *Br J Ophthalmol*. 2000;84:741–745.
62. Greenberg JP, Duncker T, Woods RL, Smith RT, Sparrow JR, Delori FC. Quantitative fundus autofluorescence in healthy eyes. *Invest Ophthalmol Vis Sci*. 2013;54:5684–5693.
63. Burke TR, Duncker T, Woods RL, et al. Quantitative fundus autofluorescence in recessive Stargardt disease. *Invest Ophthalmol Vis Sci*. 2014;55:2841–2852.

Investigative Ophthalmology & Visual Science

64. Duncker T, Tsang SH, Lee W, et al. Quantitative fundus autofluorescence distinguishes ABCA4-associated and non-ABCA4-associated bull's-eye maculopathy. *Ophthalmology*. 2015;122:345–355.

65. Eandi CM, Nassisi M, Lavia C, Alovisi C, de Sanctis U. Macular pigment density and quantitative fundus autofluorescence in young healthy subjects. *Invest Ophthalmol Vis Sci*. 2017;58:2284–2290.

Investigative Ophthalmology & Visual Science